ORIENTAL JOURNAL OF CHEMISTRY
An International Open Access, Peer Reviewed Research Journal
www.orientjchem.org
ISSN: 0970-020 X
CODEN: OJCHEG
2026, Vol. 42, No.(4):
Pg. 1560-1573

EGFR-Targeted Amino Quinoxaline Derivatives as Potential Anticancer Interventions: in silico design and in vitro evaluations

H. ABITHA[1,2] and D. KUMUDHA[1]*

[1]Faculty of Pharmacy, Karpagam Academy of Higher Education, Coimbatore-641021, Tamil Nadu, India
[2]Department of Pharmaceutical Chemistry, Nehru College of Pharmacy, Thrissur-680588, Kerala, India.
*Corresponding author E-mail: drkumudha.d@kahedu.edu.in

http://dx.doi.org/10.13005/ojc/420427

(Received: April 09, 2026; Accepted: June 05, 2026)

ABSTRACT

The Epidermal Growth Factor Receptor (EGFR) remains validated therapeutic goal for Breast Cancer, especially because of its function in signalling pathways that promote tumor development and viability. In the current investigation, a series of newly designed amino quinoxaline derivatives (QN1–QN10) were investigated for their potential EGFR inhibitory and anticancer activities using an integrated in silico and in vitro approach. Molecular docking studies were carried out using Schrödinger Maestro to rate the binding kinetics of the designed compounds with the EGFR tyrosine kinase domain (PDB ID: 4HJO), employing erlotinib as the reference standard. The docking protocol was validated by redocking erlotinib into the active site, confirming the reliability of the methodology. Glide extra-precision (XP) docking revealed favourable binding orientations of selected derivatives within the EGFR catalytic pocket. The cytotoxicity of selected compounds (QN2, QN4, and QN8) was further calculated through MTT assay for human breast cancer cell line MCF-7. The results proved that the cell longevity was decreased in a concentration-dependent way, with erlotinib exhibiting the greatest potency (LC50 = 18.47 µg/mL). Among the synthesized derivatives, QN4 showed relatively higher activity (LC50 = 121.52 µg/mL) than QN2 and QN8. Statistical analysis proved the relevance of the cytotoxic effects observed ($p < 0.0001$). Overall, the combined computational and biological findings suggest that amino quinoxaline scaffolds indicate potential avenues for enhanced optimization as EGFR-targeted anticancer drugs.

Keywords: EGFR, Quinoxaline derivatives, Molecular docking, MTT assay, Breast cancer, Erlotinib.

INTRODUCTION

Breast cancer is most profoundly prevalent carcinoma and the primary reason for cancer mortality among women globally. The disease complexity and drug resistance remain key clinical issues despite substantial advances in early identification and systemic therapies. Breast cancer

is generally classified according to the expression status of hormone receptors like progesterone and estrogen receptors and Human Epidermal Growth Factor Receptor 2 (HER2). Triple-negative breast cancer (TNBC) is one of the subtypes among them, accounting for 15–20% of all breast cancer, and characterized by aggressive clinical symptom behaviour, early tumor growth and unfavourable outcomes due to the absence of normal levels of ER, PR, and HER2 [1-4].

Cancer treatment is the principal therapy for TNBC as it lacks well-defined molecular targets, in contrast to hormone receptor-positive or HER2-amplified breast tumors. According to new research, a significant portion of TNBC cases had high expression and excessive induction of EGFR, indicating that EGFR-driven signalling pathways have a role in tumor development, survival and attack. Therefore, in aggressive forms of breast cancer, EGFR is a desirable therapeutic target for the creation of new small-molecule inhibitors[5-8].

In medicinal chemistry, quinoxaline is a special heterocyclic scaffold with a wide range of pharmacological actions, such as kinase inhibition, redox modulation, and anticancer effects. Receptor binding affinity and biological activity can be significantly increased by structurally altering the quinoxaline nucleus, especially by amino and hydrazinyl replacements. In order to find and evaluate new amino quinoxaline derivatives as possible EGFR targeted anticancer medicines against breast cancer, the current study uses a rational drug design method that includes molecular docking, synthetic chemistry and in vitro biological monitoring[9-10].

MATERIALS AND METHODS

Designing and synthesis of new leads

The parent quinoxaline nucleus was used as a flexible scaffold to create a new ligand that targets EGFR because of its aromatic, planar structure and capacity to form stable connections within the kinase domain's ATP-binding site. In order to replicate the hinge-binding interactions of common EGFR inhibitors like erlotinib, structural alterations were made at strategic points along the quinoxaline ring. These included hydrogen bonding with the crucial Met793 residue and the addition of additional substituents to occupy nearby hydrophobic pockets and solvent-exposed areas in order to improve affinity and selectivity[11].

In addition to increasing binding potency, these customized alterations provided structural flexibility to get around resistance brought on by gatekeeper mutations like T790M. Therefore, a promising platform for creating a strong compound with ideal pharmacophoric features for efficient EGFR inhibition was offered by the quinoxaline-based framework[12].

Designing of ten amino derivatives of 2-[(2E)-2-benzylidenehydrazinyl]-3-quinoxaline was done. 3-Chloro-2-hydrazinyl quinoxaline on condensation with benzaldehyde in the presence of acetic acid and ethanol to yield N-[(E)-benzylidene amino]-3-chloro-quinoxalin-2-amine. The resulting Schiff base intermediate was subsequently reacted with ten different amino derivatives (Table 1) in DMSO and triethylamine (TEA) with elimination of HCl to afford the target compounds — amino derivatives of 2-[(2E)-2-benzylidenehydrazinyl]-3-quinoxaline (Figure. 1).

Intermediate N-[(E)-benzylidene amino]-3-chloro-quinoxalin-2-amine synthesis

The current study generated the best docked amino quinoxaline derivatives based on molecule-to-molecule docking results. 3-chloro-

Table 1: Different amino derivatives used in the study

Code for designed molecules	Amino derivatives
QN1	pyridin-2-amine
QN2	pyridin-4-amine
QN3	pyrimidin-2-amine
QN4	6-methylpyrimidin-4-amine
QN5	methyl 2-aminopyrimidine-5-carboxylate
QN6	pyrimidin-4-amine
QN7	1,3-dihydro-2H-isoindol-2-amine
QN8	5-amino-1H-isoindole-1,3(2H)-dione
QN9	2-hydrazinyl-1,3-benzothiazole
QN10	6-methoxy-1,3-benzothiazol-2-amine

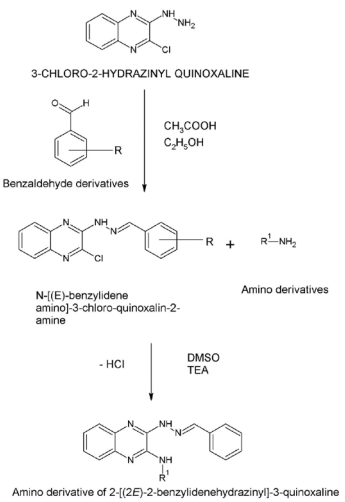

Fig. 1: Shows the designed scheme for the synthesis of novel amino derivatives of benzylidene quinoxaline derivatives

2-hydrazinyl quinoxaline was first concentrated with benzaldehyde in ethanol using catalytic acetic acid. Refluxing the reaction mixture for an appropriate period of time produced the corresponding Schiff base intermediate, N-[(E)-benzylidene amino]-3-chloro-quinoxalin-2-amine. The crude product was purified by recrystallization, and the reaction's progress was monitored using thin-layer chromatography[13–17].

QN2: 3-[(2E)-2-benzylidenehydrazinyl]-N-(pyridin-4-yl) quinoxalin-2-amine

The synthesized Schiff base intermediate was subsequently reacted with 4-amino pyridine in the presence of triethylamine (TEA) using dimethyl sulfoxide (DMSO) as solvent. The target amino quinoxaline derivatives were obtained through nucleophilic substitution and hydrogen chloride elimination. The final compounds were obtained in good yield by filtering, washing, and drying the precipitated solid after the reaction mixture was added to ice-cold water.

QN4: 3-[(2E)-2-benzylidenehydrazinyl]-N-(6-methylpyrimidin-4-yl) quinoxalin-2-amine

The synthesized Schiff base intermediate responded with 4-amino-6-methyl pyramidine in an environment of triethylamine (TEA) and dimethyl sulfoxide (DMSO) as solvent. The reaction proceeded through nucleophilic substitution with loss of hydrogen chloride to give the desired amino quinoxaline derivatives. The resultant mixture was poured into ice-cold water, and the solid obtained was filtered, washed and dried to give a high yield of the final product.

QN8: 5-({3-[(2E)-2-benzylidenehydrazinyl] quinoxalin-2-yl} amino)-1H-isoindole-1,3(2H)-dione

The synthesized Schiff base intermediate mixed with 5-amino-1H-isoindole-1,3(2H)-dione in triethylamine (TEA) and dimethyl sulfoxide (DMSO) as solvent. The reaction was carried out by nucleophilic substitution with elimination of hydrogen chloride to give the target amino quinoxaline derivatives The resulting product generated was blended into ice-cold water and the solid was purified off and rinsed and evaporated to give the end product with better yield[18-22].

Molecular Docking Studies

Structure-based molecular docking helps to examine the binding capacity and kinetic interactions characteristics of the generated quinoxaline derivatives with an EGFR tyrosine kinase structure. The crystallographic framework of EGFR along erlotinib (PDB ID: 4HJO) downloaded from Protein Data Bank and use Schrödinger Maestro's Protein Preparation Wizard to get ready. Protein preparation comprised the removal of crystallographic water molecules, the insertion of hydrogen atoms, correction of bond orders, and energy minimization to obtain a stable receptor conformation.

Ligands were prepared using the LigPrep module, generating three-dimensional geometries, appropriate ionization states, and optimized conformations suitable for docking. The receptor grid was generated by centering on the co-crystallized ligand erlotinib, thereby defining the ATP-binding catalytic pocket of EGFR.

Docking simulations were carried out using Glide extra-precision (XP) mode. Erlotinib was used as the reference inhibitor and redocked into the EGFR active site to validate the docking protocol. The designed compounds were then docked, and their binding poses and docking scores were analysed. Among the series, compounds QN2, QN4, and QN8 demonstrated favourable docking scores and stable interactions within the EGFR

binding pocket, while erlotinib exhibited a marginally higher docking score, consistent with its established inhibitory potency. Based on these results, QN2, QN4, and QN8 were selected for chemical synthesis and further biological evaluation[23-26].

DPPH radical scavenging assay

0.1 mm DPPH solution (4 mg in 100 ml ethanol) was mixed with samples (25–400 µg/ml) and DMSO as a reference, the samples were incubated in the dark for 20 minutes before the absorbance at 517 nm was recorded. The percentage inhibition was computed as

$$\left[\frac{\text{control-test}}{\text{control}}\right]100$$

Table 2: Molecular Docking Scores of Standard Drug and Quinoxaline Derivatives Against EGFR

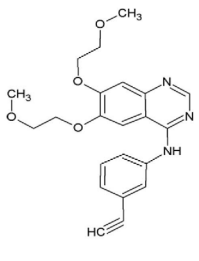		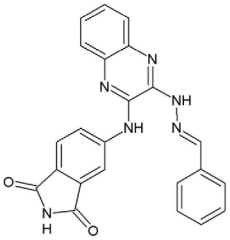		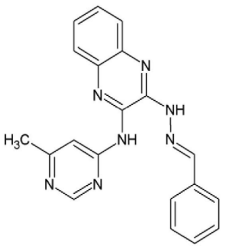	
Title	STANDARD	Title	QN8	Title	QN4
Docking score	-9.501	Docking score	-9.305	Docking score	-8.728
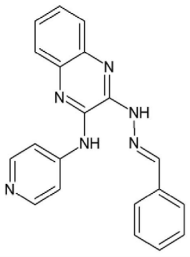		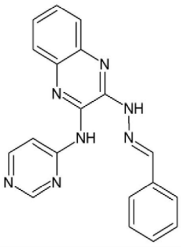		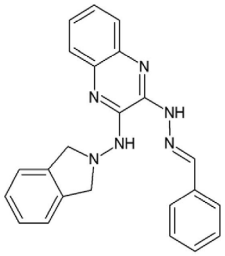	
Title	QN2	Title	QN6	Title	QN7
Docking score	-8.063	Docking score	-8.031	Docking score	-6.651
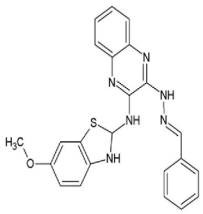		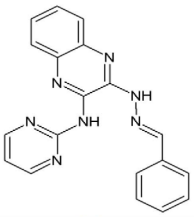		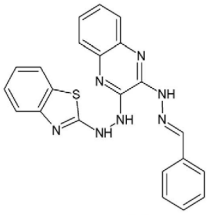	
Title	QN10	Title	QN3	Title	QN9
Docking score	-6.332	Docking score	-6.222	Docking score	-6.066
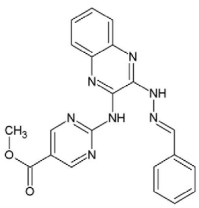		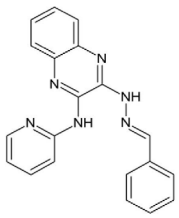			
Title	QN5	Title	QN1		
Docking score	-5.575	Docking score	-4.772		

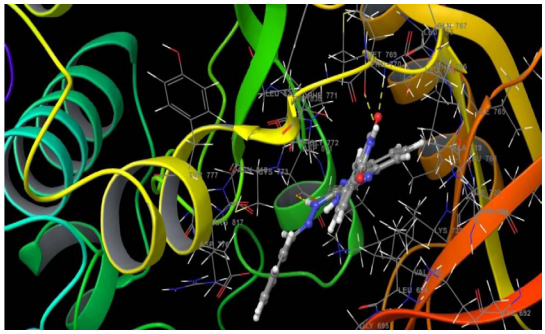

Fig. 2: 3D binding interaction of QN8 with the protein EGFR

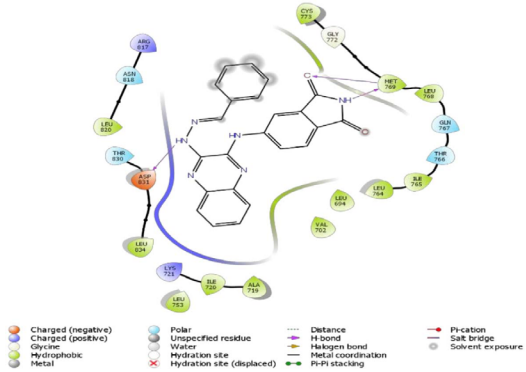

Fig. 3: Binding interaction of QN8 with the protein EGFR

Fig. 4: 3D binding interaction of the standard erlotinib with the protein EGFR

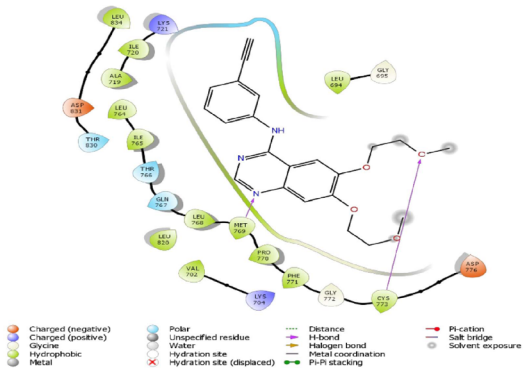

Fig. 5: Binding interaction of the standard erlotinib with the protein EGFR

In-vitro anticancer effect determination by MTT assay

MCF-7 cells were grown at 37°C in an incubator with 5% CO2 in DMEM enriched with 10% FBS and antibiotics. A 96-well plate was introduced with cells (5×10^3 cells/well) and cultured for 24 hours. Untreated cells were treated as a reference, and test chemicals produced in 0.1% DMSO were added at doses of 6.25–100 µg/ml and incubated for 48 hours. Cells were examined under a microscope for changes in morphology subsequent maturation. Each well was then filled with 30 µl of MTT solution, and the mixture was incubated for 4 hrs. A microplate reader was used to calculate absorbance at 540 nm after the formazan crystals were completely dissolved in DMSO. Growth inhibition as a percentage was calculated as:

$$\left[\frac{\text{Mean OD Samples}}{\text{Mean OD of control group}}\right]100$$

RESULTS AND DISCUSSION

Molecular Docking Analysis

Docking studies revealed that the designed quinoxaline derivatives effectively occupied an ATP-binding pocket of EGFR tyrosine kinase domain[10]. speculated compounds' docking scores are listed in Table 2. Key interactions observed included π–π stacking, hydrophobic interactions, and hydrogen bonding with vital amino acids residues within the active site which is depicted in Figures 2, 3, 4 and 5 as the binding interaction of the designed molecule QN8 and standard Erlotinib. The binding orientation of selected compounds was comparable to that of erlotinib, supporting their potential as EGFR inhibitors.

Several developed compounds showed good binding affinities similar to the standard

Erlotinib (–9.501 kcal/mol), according to the docking results. The top three compounds (–9.305, –8.728, and –8.063 kcal/mol) were chosen for additional production and biological analysis because they showed strong interactions with the target protein.

The three compounds with the best docking scores and interaction profiles were chosen for synthesis out of the 10 proposed compounds. In order to make effective use of time and resources, this prioritizing was based on their anticipated binding affinity toward the target protein. In early-stage drug research, this method is frequently used to find intriguing lead candidates.

Chemistry

QN2: 3-[(2E)-2-benzylidenehydrazinyl]-N-(pyridin-4-yl) quinoxalin-2-amine.

Yellowish-brown solid; MF: $C_{20}H_{16}N_6$; MW: 340.38 (g/m); mp: 255–257 °C; Yield: 72%; FT-IR (cm ^{1}): 3498 (N–H stretching, hydrazine and secondary amine), 1614 (C=N stretching, azomethine and quinoxaline), 3049 (aromatic C–H), 1269 (C–N stretching), and 1578 (aromatic C=C). 1H NMR (400 MHz): δ 7.18-7.46 (5H, 7.25 (tt, J = 7.4, 1.3 Hz), 7.36 (dddd, J = 7.9, 7.4, 1.9, 0.5 Hz), 7.40 (dddd, J = 7.9, 1.5, 1.3, 0.5 Hz), 7.60-7.76 (ddd, J = 7.7, 7.2, 1.8 Hz)), and 7.86-8.09 (ddd, J = 5.3, 1.8 Hz).13C NMR: δ 110.2, 127.8, 128.1, 128.7, 129.3-129.4, 129.3, 130.8-130.9, 130.8, 133.7, 141.4-141.6, 141.5, 141.8, 142.4, 150.3, 154.8-155.0. MS (ESI):m/z [M] : 340.

QN4: 3-[(2E)-2-benzylidenehydrazinyl]-N-(6-methylpyrimidin-4-yl) quinoxalin-2-amine

Yellowish-brown solid; MF: $C_{21}H_{18}N_8$MW: 382.42 (g/m); mp: 250–252 °C; Yield: 74%. FT-IR (cm ^{1}): 1604 (C=N stretching, azomethine and quinoxaline), 1530 (aromatic C=C stretching), 1268 (C–N stretching), 3041 (aliphatic C–H, methyl group), and 3356 (N–H stretching, hydrazine and secondary amine). 1H NMR (400 MHz): δ 2.59 (3H, s), 6.83 (1H, d, J = 0.4 Hz), 7.18-7.46 (5H, 7.25 (tt, J = 7.4, 1.3 Hz), 7.36 (dddd, J = 7.9, 7.4, 1.9, 0.5 Hz), 7.40 (ddd, J = 7.9, 1.5, 1.8 Hz), 7.61-7.77 (ddd, J = 7.7, 7.2, 1.9 Hz)).13C NMR: 24.6, 103.8, 127.8, 128.1, 128.7, 129.3-129.4, 130.8-130.9, 133.7, 141.4-141.6, 142.4, 154.0, 154.8-155.0, 157.4, 158.4. MS (ESI):m/z [M+1] : 356.

QN8: 5-({3-[(2E)-2-benzylidenehydrazinyl] quinoxalin-2-yl} amino)-1H-isoindole-1,3(2H)-dione.

Brown solid; MF: $C_{23}H_{16}N_6O_2$; MW: 408.41 (g/m); mp: 270-272 0C; Yield: 78%; FT-IR (cm 1): 1637 (asymmetric and symmetric imide C=O), 3361 (N–H, hydrazine), 1604 (C=N, azomethine), 1546 (aromatic C=C), 1269 (C–N). 1H NMR (400 MHz): δ 7.06-7.46 (6H, 7.12 (dd, J = 7.8, 1.4 Hz), 7.25 (tt, J = 7.4, 1.3 Hz), 7.36 (dddd, J = 7.9, 7.4, 1.9, 0.5 Hz), 7.40 (dddd, J = 7.9, 1.5, 1.3, 0.5 Hz)), 7.61-7.86 (3H, 7.68 (ddd, J = 7.6, 7.2, 1.8 Hz), 7.70 (ddd, J = 7.7, 7.2, 1.8 Hz), 7.80 (dd, J = 7.8, 0.5 Hz)), 7.89-8.09 (4H, 7.94 (s), 8.00 (dd, J = 1.4, 0.5 Hz), 8.01 (ddd, J = 7.7, 1.8, 0.5 Hz), 8.03 (ddd, J = 7.6, 1.8, 0.5 Hz)). 13C NMR: δ 116.0-116.1,

Table 3: Percentage of inhibition computed for drugs QN2, QN4, QN8, and conventional Erlotinib

Concentrations (μg/ml)	Absorbance	Percentage of inhibition
Control	0.714	0.0000
25	0.354	50.4202
50	0.245	65.6863
100	0.195	72.6891
200	0.125	82.4930
400	0.046	93.5574
Sample Code: QN2		
Control	0.714	0.0000
25	0.445	37.6751
50	0.387	45.7983
100	0.318	55.4622
200	0.263	63.1653
400	0.212	70.3081
Sample Code: QN4		
Control	0.714	0.0000
25	0.655	8.2633
50	0.612	14.2857
100	0.565	20.8683
200	0.495	30.6723
400	0.421	41.0364
Sample Code: QN8		
Control	0.714	0.0000
25	0.504	29.4118
50	0.414	42.0168
100	0.313	56.1625
200	0.252	64.7059
400	0.201	71.8487

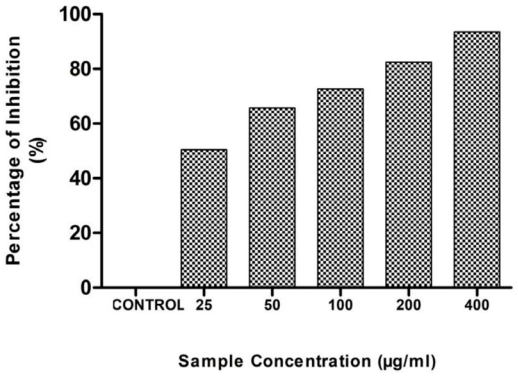

Fig. 6: DPPH radical scavenging test in Standard

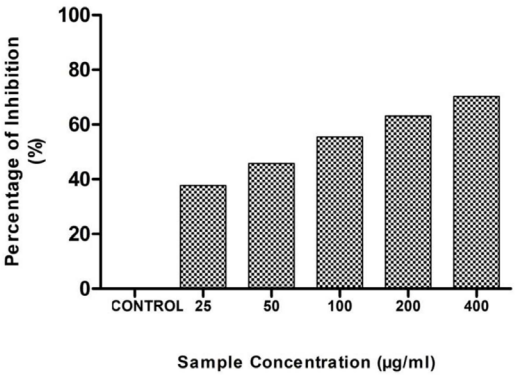

Fig. 7: DPPH radical scavenging test in QN2

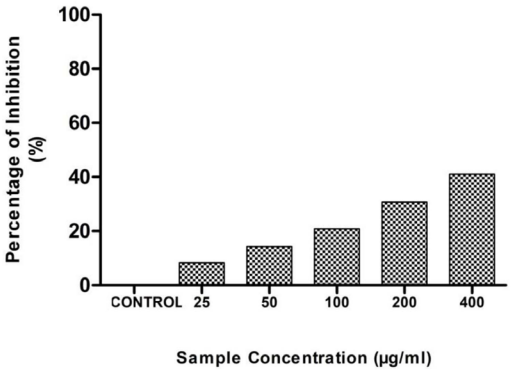

Fig. 8: DPPH Radical scavenging test in QN4

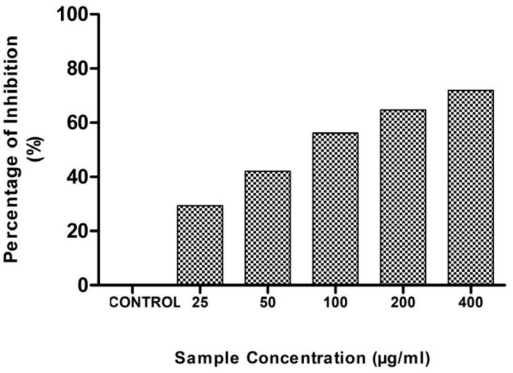

Fig. 9: DPPH Radical scavenging test in QN8

125.2, 127.8, 128.1, 128.7, 129.3-129.4, 129.3, 130.8-130.9, 132.5, 133.7, 136.4, 139.4, 141.4-141.6, 142.4, 154.8-155.0, 167.1, 168.9. MS (ESI): m/z [M+1] : 409.

DPPH radical scavenging assay

The antioxidant activity of the test substances was evaluated using the assay. The method relies on antioxidants that contribute hydrogen or electrons to reduce the stable DPPH radical, hence reducing absorption. The radical scavenging activity was compared using a standard antioxidant and expressed IC_{50} values and % inhibition. Table 3 displays the percentage of inhibition calculated for the medications QN2, QN4, QN8, and traditional Erlotinib. STANDARD: ASCORBIC ACID
Sample Code: QN2
Sample Code: QN4
Sample Code: QN8

For both the standard and quinoxaline derivatives (QN2, QN4, and QN8), the DPPH assay demonstrated a concentration-dependent rise in radical scavenging. The standard exhibited the highest activity, confirming strong antioxidant potential. Among the compounds, QN8 showed the greatest scavenging, especially at higher concentrations, indicating effective hydrogen or electron donation. QN2 had moderate activity with a steady increase, while QN4 displayed the lowest inhibition. Overall, antioxidant efficacy ranked as Standard > QN8 > QN2 > QN4, highlighting structural effects on scavenging ability. Figures 6–9 demonstrate the conventional and produced compounds' DPPH radical scavenging abilities.

The DPPH radical scavenging effectiveness of the standard and the produced quinoxaline derivatives may be quantitatively compared using

the IC_{50} values obtained from the graphical data. As a positive control for comparison, the standard had the lowest IC_{50} value (24.719 µg/ml), showing significant antioxidant activity. QN2 (74.6757 µg/ml) and QN8 (78.2403 µg/ml) demonstrated similar IC_{50} values among the test compounds, indicating a moderate capacity to scavenge free radicals. Compared to QN4, its comparatively lower IC_{50} values indicate superior hydrogen or electron-donating capabilities. Conversely, QN4 showed a significantly larger IC_{50} value (455.046 µg/ml), which suggests that it has poor antioxidant activity and is much less effective at neutralizing DPPH radicals.

The antioxidant efficacy was generally in the following order: Standard > QN2 ≈ QN8 > QN4. The differences in IC_{50} values amongst the produced compounds demonstrate how structural characteristics affect the effectiveness of radical scavenging. These results support the graphical analysis's concentration-dependent patterns and demonstrate that QN2 and QN8 have significant antioxidant activity while QN4 has little scavenging capacity.

The DPPH antioxidant test was used to evaluate the compounds' role to scavenge free radicals since oxidative stress results significant role in the cancer development and cell death. By lessening the negative consequences of oxidative stress, compounds with both cytotoxic and antioxidant qualities may provide therapeutic benefits.

Table 4. Percentage of growth inhibition that the medicines exhibited using the MTT assay

Sample Concentration (µg/ml)	OD I	OD II	OD III	Average Absorbance @ 540nm	Percentage Viability
Control	0.9015	0.8931	0.8876	0.8941	100.00
Sample Code: Erlotinib					
6.25	0.6524	0.6397	0.64226	0.6448	72.12
12.5	0.5628	0.5811	0.5834	0.5758	64.40
25	0.3121	0.3094	0.2974	0.3063	34.26
50	0.2234	0.2035	0.2175	0.2148	24.02
100	0.1423	0.1169	0.1358	0.1317	14.73
Sample Code: QN2					
6.25	0.7694	0.7684	0.7724	0.7701	86.13
12.5	0.7369	0.7283	0.7314	0.7322	81.89
25	0.6847	0.6997	0.7002	0.6949	77.72
50	0.6328	0.6237	0.6197	0.6254	69.95
100	0.5842	0.5796	0.5633	0.5757	64.39
Sample Code: QN4					
6.25	0.7398	0.7493	0.7521	0.7471	83.56
12.5	0.6958	0.7013	0.7006	0.6992	78.21
25	0.6258	0.6415	0.6328	0.6334	70.84
50	0.5741	0.5876	0.5793	0.5803	64.91
100	0.5126	0.5006	0.5347	0.5160	57.71
Sample Code: QN8					
6.25	0.7529	0.7516	0.7605	0.7550	84.44
12.5	0.7025	0.7156	0.7234	0.7138	79.84
25	0.6636	0.6751	0.6693	0.6693	74.86
50	0.6183	0.6324	0.6219	0.6242	69.81
100	0.5526	0.5613	0.5598	0.5579	62.40

In-Vitro Anticancer Activity (MTT Assay)

The activity of the generated compounds QN2, QN4, and QN8 against the human breast cancer cell line MCF-7 was evaluated using the MTT test, with erlotinib serving as the standard reference drug. After 48 hours of exposure to increasing concentrations of the test compounds (6.25–100 µg/ml), cell viability was assessed using spectrophotometry at 540 nm.

Erlotinib's strong anticancer efficacy was confirmed by a noticeable concentration-dependent decrease in cell viability. Although they were less potent than erlotinib, the synthesized quinoxaline derivatives similarly showed dose-dependent cytotoxic effects. QN4 exhibited comparatively greater cytotoxic activity among the investigated chemicals, followed by QN8 and QN2. The observed reduction in percentage cell viability supports the anticancer potential of the suggested amino quinoxaline derivatives. Furthermore, Table 4 lists the percentage of growth inhibition that the medicines exhibited using the MTT assay.

The graphical representation of the MTT assay findings for erlotinib, QN2, QN4, and QN8, respectively, is shown in Figures 10-13. The X-axis shows different sample concentrations (6.25–100 µg/ml), and the percentage of viability of cells is displayed on the Y-axis. For every drug, a pronounced dose-dependent decline in cell viability was noted. The assay technique was validated by the maximum cytotoxic activity shown by erlotinib. The produced compounds' anticancer potential was confirmed by their constant decline in viability as concentration increased.

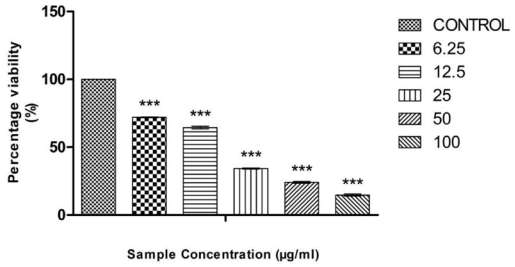

Fig. 10: Standard Erlotinib evaluated by MTT assay

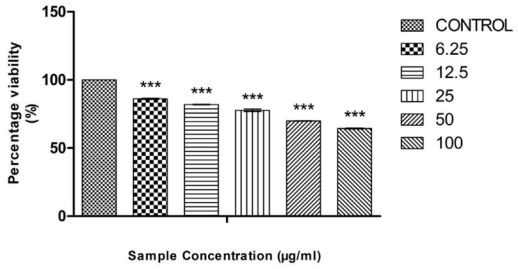

Fig. 11: QN2 evaluated by MTT assay

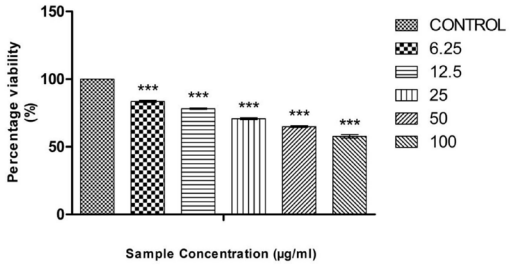

Fig. 12: QN4 evaluated by MTT assay

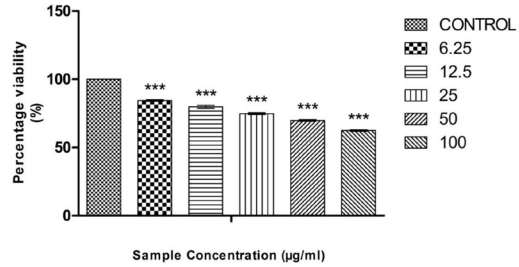

Fig. 13: QN8 evaluated by MTT assay

Erlotinib exhibited a markedly lower LC_{50} value (18.47 µg/ml), confirming its strong cytotoxic activity and validating the reliability of the assay conditions. In contrast, the tested derivatives QN2, QN4, and QN8 showed higher LC_{50} values of 156.26, 121.52, and 150.51 µg/ml, respectively, suggesting comparatively moderate cytotoxic effects. Among the synthesized compounds, QN4 demonstrated relatively better activity, as evidenced by its lower LC_{50} value, indicating enhanced cellular growth inhibition compared to QN2 and QN8. Although the derivatives did not surpass the standard drug in potency, their measurable cytotoxicity supports

their potential as lead molecules for further structural optimization. The variation in LC_{50} values may be attributed to differences in substituent effects influencing EGFR binding affinity and cellular uptake.

Comparative analysis of QN2, QN4, and QN8 phase contrast pictures

Cells treated with quinoxaline derivatives QN2, QN4, and QN8 showed concentration-dependent morphological alterations in comparison to the untreated control, as shown by phase contrast microscopy analysis. The control cells had a well-spread spindle form, great confluency, and normal morphology with intact membranes. Reduced levels (6.25 and 12.5 µg/ml) of QN2-treated cells exhibited moderate morphological changes, with gradual rounding, decreased cell density, and partial loss of adherence seen at 25 µg/ml. At 50 and 100 µg/ml, however, there was noticeable cell shrinkage and detachment. On the other hand, QN4 caused more noticeable morphological alterations at comparable doses, such as an early loss of cell-cell contact, more abnormalities in the membrane, and a significant decrease in

The concentration-dependent cytotoxicity found was in agreement with the general order of QN4 > QN2 > QN8 for severity of morphological damage.

Phase-contrast microscopy photos of cells treated with erlotinib, QN2, QN4 and QN8, revealing morphological alterations generated by the treatments, are shown in Figs. 14-17. An assessment of the treatments with the untreated control showed clear differences in cell density, morphology and adherence, indicating differences in cytotoxicity.

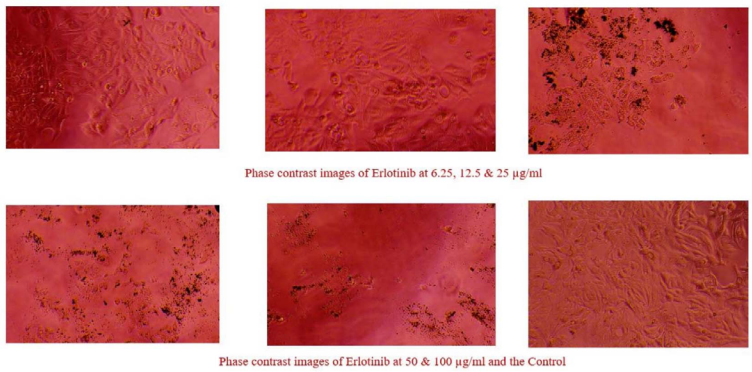

Fig. 14: Erlotinib-treated cells

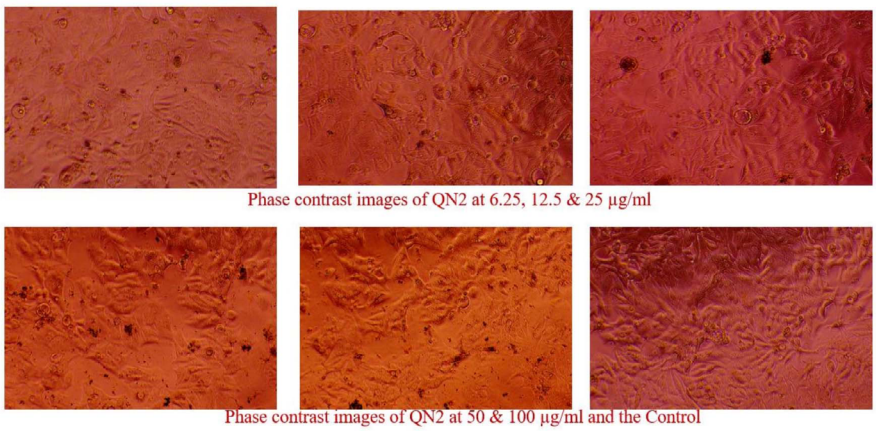

Fig. 15: QN2-treated cells

In the current research, rational structure-oriented methodology proved effective to design, synthesize and biological assessment of new amino substituted quinoxaline derivatives as possible targets for EGFR modulation in breast cancer treatment. The quinoxaline scaffold was chosen as a planar aromatic structure with probable interactions with key hinge area residues in the EGFR kinase domain. Molecular docking investigations revealed that several of produced derivatives efficiently occupied the ATP-binding pocket of EGFR, exhibiting important hydrogen bonding, hydrophobic interactions, and π–π stacking similar to that of the therapeutically employed inhibitor erlotinib.

The QN2, QN4 and QN8 compounds of the planned series showed good docking scores and stable binding conformations which justified the selection of these compounds for chemical production. Spectral assessment proved the production of the desired compounds. In-vitro examination in opposition to MCF-7 breast cancer cell line demonstrated among produced compounds showed the dose-dependent cytotoxic effects. QN4 was the most active derivative among the created compounds but less potent than erlotinib. The observed differences in biological activity are due to the substituent-dependent modification of EGFR binding affinity and cellular permeability. In vitro cytotoxicity and molecular docking results seemed to be in conflict. One compound provided the best docking score, however another molecule

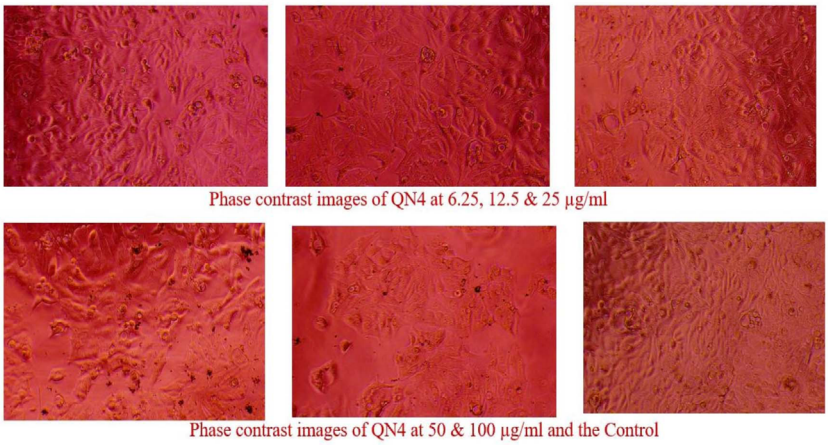

Fig. 16: QN4-treated cells

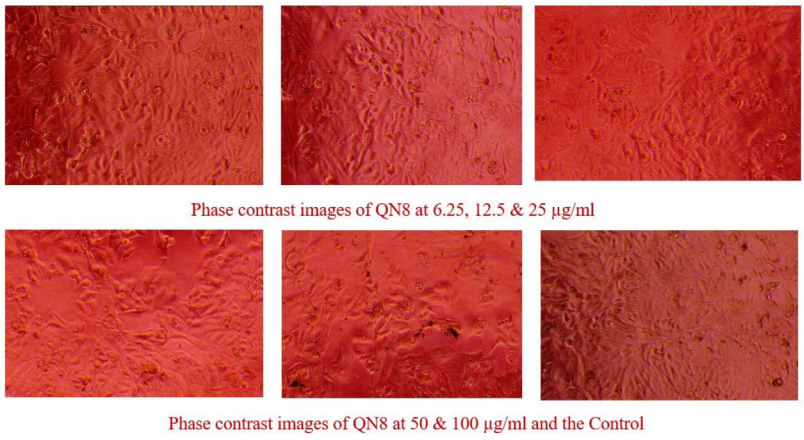

Fig. 17: QN8-treated cells

demonstrated considerably higher activity against the MCF-7 cell line studies. This lack of direct connectivity could be explained by the intrinsic limitation of molecular docking that mainly predicts the binding affinity of molecules toward a certain target under idealized conditions.

Cytotoxic activity in biological systems is affected by many factors, including membrane permeability, solubility, metabolic stability and off-target interactions. Therefore, even if a drug shows a high docking score, it does not mean that it exhibits the highest biological activity when it has poor physicochemical or pharmacokinetic properties. Conversely, medicines with intermediate docking scores may demonstrate enhanced cytotoxicity due to higher cellular uptake or novel mechanisms of action. Therefore, the docking data should be considered predictive and useful, not definitive. More studies are required to establish a clear link between binding affinity and biological activity.

Limitations

One of the drawbacks of the study is the modest cytotoxic activity of the generated compounds. Potency and selectivity need to be improved by further structural modification and detailed biological evaluation. Furthermore, although antioxidant activity was assessed, there is currently limited evidence of a direct relationship between it and EGFR inhibition, which requires further investigation.

CONCLUSION

Among the amino derivatives, the 5-amino-1H-isoindole-1,3(2H)-dione derivative QN8 exhibited the greatest EGFR binding affinity, modest antioxidant activity and cell toxicity. The MTT assay indicated higher cytotoxicity for QN4, yet it had a weak antioxidant profile and a lower docking score, indicating non-specific toxicity. Antioxidant QN2 showed decreased EGFR interaction. QN8 is an electron rich indole dione and may interact more successfully with the target enzyme. QN2 and QN4 were both pyridine and pyrimidine derivatives. As a result, QN8 was the most efficient and selective lead chemical targeting EGFR. The synthesized quinoxaline derivatives were established as feasible lead compounds due to their consistent EGFR directed binding behaviour and statistically significant cytotoxicity, although not more potent than the reference medication in terms of antiproliferative activity. These results establish a strong basis for additional structural optimization, mechanistic research, and further biological evaluation including kinase inhibition assays and testing against resistant EGFR mutants. Together, our work supports the promise of quinoxaline-based frameworks as versatile scaffolds for the design of next generation EGFR-targeted anticancer medicines. The proposed EGFR inhibitory activity, as shown by preliminary cytotoxic evaluation and molecular docking predictions, has to be further experimentally validated by molecular and biochemical studies.

ACKNOWLEDGEMENTS

The authors gratefully acknowledge CRMAS Research Laboratory for supplying the technical assistance and research facilities required to finish this endeavour successfully. Additionally, the authors express their gratitude to the CRMAS Research personnel for their help with instrumental and analytical research.

REFERENCES

1. Siegel RL, Miller KD, Jemal A. Cancer statistics, 2024. *CA Cancer J Clin*. **2024**;*74(1):*17–48. https://doi.org/10.3322/caac.21763
2. Perou CM, Sørlie T, Eisen MB, van de Rijn M, Jeffrey SS, Rees CA, et al. Molecular portraits of human breast tumours. *Nature.* **2000**; *406(6797):*747–52. https://doi.org/10.1038/35021093
3. Carey LA, Perou CM, Livasy CA, Dressler LG, Cowan D, Conway K, et al. Race, breast cancer subtypes, and survival in the Carolina Breast Cancer Study. JAMA. **2006**;*295(21):*2492–502. https://doi.org/10.1001/jama.295.21.2492
4. Foulkes WD, Smith IE, Reis-Filho JS. Triple-negative breast cancer. *N Engl J Med.* **2010;** *10(5):* 321–34. https://doi.org/10.1056/NEJMra1001389

5. Bianchini G, Balko JM, Mayer IA, Sanders ME, Gianni L. Triple-negative breast cancer: challenges and opportunities of a heterogeneous disease. *Nat Rev Clin Oncol.* **2016***;13(11):*674–90. https://doi.org/10.1038/nrclinonc.2016.66
6. Nielsen TO, Hsu FD, Jensen K, Cheang M, Karaca G, Hu Z, et al. Immunohistochemical and clinical characterization of the basal-like subtype of invasive breast carcinoma. Clin *Cancer Res*. **2004***;10(16):*5367–74. https://doi.org/10.1158/1078-0432.CCR-04-0220
7. Hynes NE, Lane HA. ERBB receptors and cancer: the complexity of targeted inhibitors. *Nat Rev Cancer.* **2005***;5(5):*341–54. https://doi.org/10.1038/nrc1609
8. Zhang H, Berezov A, Wang Q, Zhang G, Drebin J, Murali R, et al. ErbB receptors: from oncogenes to targeted cancer therapies. *J Clin Invest.* **2007**;*117(8*) :2051–58. https://doi.org/10.1172/JCI32278
9. Carta A, Corona P, Loriga M. Quinoxaline 1,4-dioxide: a versatile scaffold endowed with manifold pharmacological activities. *Curr Med Chem.* **2005**;*12(19):*2259–72. https://doi.org/10.2174/0929867054637697
10. Pingaew R, Prachayasittikul V. Quinoxaline-based anticancer agents: a review. *Eur J Med Chem.* **2016**; *118:*130–69. https://doi.org/10.1016/j.ejmech.2016.04.040
11. Alessandra C Pinheiro, Thais C Mendonça Nogueira, Marcus V N de Souza. Quinoxaline Nucleus: A Promising Scaffold in Anti-cancer Drug Discovery. *Anticancer Agents Med Chem*. **2016**; *16(10):* 1339-52. doi: 10.2174/1871520616666160622090839.
12. Yuyang Ding , Xiaoqian Xue. Medicinal Chemistry Strategies for the Modification of Bioactive Natural Products. *Molecules.* **2024***; 29(3):*689. doi: 10.3390/molecules29030689
13. Carta A, Loriga M, Paglietti G, Mattana A, Fiori PL, Mollicotti P. Synthesis and biological evaluation of quinoxaline derivatives as antimicrobial agents. *Eur J Med Chem.* **2004***;39(2*):195–203. https://doi.org/10.1016/j.ejmech.2003.11.009
14. Pingaew R, Prachayasittikul V. Synthesis and biological evaluation of quinoxaline-based Schiff bases as anticancer agents. *Eur J Med Chem*. **2016**; *118*:130–69. https://doi.org/10.1016/j.ejmech.2016.04.040
15. El-Gazzar AB, Hussein HA, Hafez HN. Synthesis of novel quinoxaline derivatives and evaluation of their anticancer activity. *Bioorg Med Chem*. **2009**;*17(13):*4375–82. https://doi.org/10.1016/j.bmc.2009.04.046
16. Rollas S, Küçükgüzel SG. Biological activities of hydrazone derivatives. Molecules. **2007**;*12(8):*1910–39. https://doi.org/10.3390/12081910
17. Abdel-Aziz M, Gamal-Eldeen AM, El-Sayed AM. Design, synthesis, and anticancer activity of novel quinoxaline derivatives. *Arch Pharm Chem Life Sci.* **2011**;344(7):394–405. https://doi.org/10.1002/ardp.201000290
18. El-Gazzar AB, Youssef MM, Youssef AM, Abu-Hashem AA, Badria FA. Design and synthesis of novel quinoxaline derivatives as potential anticancer agents. Eur J Med Chem. **2009**;*44(2):*609–24. https://doi.org/10.1016/j.ejmech.2008.03.031
19. Abdel-Aziz M, Gamal-Eldeen AM, El-Sayed AM. Design, synthesis and anticancer activity of novel quinoxaline derivatives. Arch Pharm *Chem Life Sci.* **2011**;*344(7):*394–405. https://doi.org/10.1002/ardp.201000290
20. Carta A, Paglietti G, Loriga M, Zanetti S, Sechi L. Quinoxaline derivatives: synthesis and biological evaluation. *Eur J Med Chem.* **2002**;*37(4*):355–66. https://doi.org/10.1016/S0223-5234(02)01352-9
21. Katritzky AR, Rees CW, Scriven EFV, editors. Comprehensive Heterocyclic Chemistry II. Oxford: Pergamon Press; **1996**.
22. Vogel AI. Vogel's Textbook of Practical Organic Chemistry. 5th ed. London: Longman Scientific & Technical; **1989**.
23. Stamos J, Sliwkowski MX, Eigenbrot C. Structure of the epidermal growth factor receptor kinase domain alone and in complex with a 4-anilinoquinazoline inhibitor. *J Biol Chem.* **2002**; *277(48):* 46265–72. https://doi.org/10.1074/jbc.M207135200
24. Yun CH, Mengwasser KE, Toms AV, Woo MS, Greulich H, Wong KK, et al. The T790M mutation in EGFR kinase causes drug resistance by increasing the affinity for ATP. Proc Natl Acad Sci U S A. **2008**;*105(6):*2070–75. https://doi.org/ 10.1073/pnas.0709662105
25. Park JH, Liu Y, Lemmon MA, Radhakrishnan

R. Erlotinib binds both inactive and active conformations of EGFR tyrosine kinase domain. *Biochem J.* **2012;** *448(3*): 417–23. https://doi.org/ 10.1042/BJ20120604

26. Friesner RA, Murphy RB, Repasky MP, Frye LL, Greenwood JR, Halgren TA, et al. Extra precision Glide: docking and scoring incorporating a model of hydrophobic enclosure for protein–ligand complexes. *J Med Chem*. **2006**;*49(21):*6177–96. https://doi.org/ 10.1021/jm0512560
27. Chang ST, Wu JH, Wang SY, Kang PL, Yang NS, Shyur LF. Antioxidant activity of extracts from Acasia confuse bark and heartwood. *J Agric Food Chem.* **2001**;49:3420-3424. https://doi.org/ 10.1021/jf0100907
28. Jerard C, Michael BP, Chenicheri S, Vijayakumar N, Ramachandran R. Rosmarinic acid-rich fraction from Mentha arvensis synchronizes Bcl/Bax expression and induces G0/G1 arrest in hepatocarcinoma cells. *Proc Natl Acad Sci India Sect B Biol Sci***. 2020***; 90*:515–522. https://doi.org/ 10.1007/s40011-019-01131-7
29. Mosmann T. Rapid colorimetric assay for cellular growth and survival: Application to proliferation and cytotoxicity assays. *J Immunol Methods.* **1983**; *65*:55–63. https://